



Published in final edited form as:

*Otol Neurotol.* 2010 April ; 31(3): . doi:10.1097/MAO.0b013e3181c99524.

## Radiographic anatomy of the infracochlear approach to the petrous apex for computer-assisted surgery

Randal Leung, MBBS, FRACS<sup>1</sup>, Ravi N. Samy, MD, FACS<sup>1</sup>, James L. Leach, MD<sup>2</sup>, Shanmugam Murugappan, Ph.D.<sup>1</sup>, Don Stredney, M.A.<sup>3</sup>, and Gregory Wiet, M.D.<sup>4</sup>

<sup>1</sup>Department of Otolaryngology / Head and Neck Surgery, University of Cincinnati / Cincinnati Children's Hospital Medical Center, Cincinnati, Ohio

<sup>2</sup>Department of Radiology, Cincinnati Children's Hospital Medical Center, Cincinnati, Ohio

<sup>3</sup>Ohio Supercomputer Center, Columbus, Ohio

<sup>4</sup>Ohio State University, Nationwide Children's Hospital

### Abstract

**Objective**—1) To define the surgical anatomy and dimensions of the infracochlear approach to the petrous apex through use of high resolution computed tomography (HRCT) 2) use of digitized images of cadaveric temporal bones for computer simulation of infracochlear access using the OSC/OSU temporal bone simulator

**Background**—The petrous apex is a surgically challenging area to access. Many routes have been described and used successfully in clinical practice. However, these routes have not been defined with the aim of application in computer-assisted surgery. The infracochlear approach, due to its access via a transcanal route, affords the opportunity for its potential application in minimally invasive computer-assisted surgery.

**Methods**—High resolution CT (HRCT) scans were performed on 102 cadaveric skulls (total of 204 temporal bones). Standard measurements were taken using an open source Picture Archiving and Communication System (PACS) software of the maximum height, width, and depth of the infracochlear approach. In addition, the maximum diameter of a circular fenestration that could be created in the infracochlear space without breaching the basal turn of the cochlea, internal carotid artery, or the jugular bulb was used to simulate a drill path. In addition, five temporal bone specimens (3 left, 2 right) underwent HRCT with the digitized images being used to create simulated temporal bones for infracochlear surgical access; the transcanal infracochlear approach was then performed by the same surgeon on the cadaveric bone.

**Results**—The mean height, width and depth of the infracochlear space in temporal bones with non-pneumatized petrous apices were 7.2 +/- 0.4mm, 9.4 +/- 0.8mm and 17.5 +/- 1.0mm respectively. Corresponding dimensions in pneumatized petrous apices were 7.6 +/- 0.4mm, 10.1 +/- 1.1 and 18.6 +/- 0.8mm. The mean diameter of the circular fenestra in the non-pneumatized petrous apices was 5.1 +/- 0.4mm compared to 5.7 +/- 0.6mm in pneumatized petrous pieces. This was statistically significant (Unpaired t-Test, p value = 0.04). The time to perform a simulated infracochlear approach to the petrous apex ranged from 3.1 – 12.6 minutes

---

Corresponding author Ravi N. Samy, M.D., F.A.C.S. Department of Otolaryngology / Head and Neck Surgery University of Cincinnati / Cincinnati Children's Hospital 231 Albert Sabin Way Cincinnati, OH 45267-0528 Ravi.Samy@UC.edu 513-558-4143.

**Publisher's Disclaimer:** This is a PDF file of an unedited manuscript that has been accepted for publication. As a service to our customers we are providing this early version of the manuscript. The manuscript will undergo copyediting, typesetting, and review of the resulting proof before it is published in its final citable form. Please note that during the production process errors may be discovered which could affect the content, and all legal disclaimers that apply to the journal pertain.

(mean: 6.1 minutes). The time to perform the same approach on the cadaveric bone ranged from 4.32 – 14.1 minutes (mean 9.3 minutes).

**Conclusions**—Temporal bones with pneumatized petrous apices have an overall larger infracochlear space. The mean diameter of a circular infracochlear path that would avoid damage to vital structures was sufficiently large in both pneumatized and non-pneumatized petrous apices to have a potential application as a safe approach in computer-assisted surgery. Such an application is feasible with mating of a robotic system with CT or MRI guided imagery, which is the next phase of this study.

## Introduction

The petrous apex is a surgically challenging area to access. Conditions that affect the petrous apex are uncommon; however, cystic lesions that involve this area often require only long term drainage rather than complete extirpation. Thus, many surgical approaches have been described to access this area; the route used is based predominantly on the individual patient's anatomy but also includes the patient's level of hearing, size of lesion, and symptoms. Access routes described include the transsphenoidal, middle cranial fossa, transmastoid (e.g., infralabyrinthine, transcochlear, etc.) and transcanal (infracochlear).<sup>1</sup>

With the advent of high-resolution imaging, virtual anatomic reconstructions, and surgical simulation, the ability to preoperatively define, plan, and practice a surgical access route through narrow anatomic corridors has been greatly enhanced. Increasingly, Computer-Assisted Surgery (CAS) has been investigated and utilized in an attempt to improve precision and accuracy where anatomic constraints dictate small and narrow operative fields.<sup>2,3</sup> The routes to the petrous apex have not been previously defined with the aim of application in CAS. The infracochlear approach, due to its access via a transcanal route as a minimally invasive approach, affords the opportunity for its potential application in CAS. In this study, we aimed to define the surgical anatomy and dimensions of the infracochlear approach to the petrous apex through use of High Resolution Computed Tomography (HRCT), in a manner that would allow translation to a computer-assisted surgical platform via use of a surgical simulator.

## Materials and Methods

The study was conducted in 2 different phases. The first phase involved the evaluation of the anatomic confines of the petrous apex. The second phase evaluated the use of the surgical simulator to perform an infracochlear approach (which was then followed by the same approach on the cadaveric specimen). The cadaveric skulls used in this study were obtained from the anatomic holdings of the Department of Pathology at the University of Cincinnati College of Medicine. For the first phase, high resolution computed tomography (HRCT) scans were performed of the cadaveric skulls with a 64-slice CT scanner (GE LightSpeed Ultra; General Electric Healthcare; Piscataway, NJ, USA) in a standardized axial plane, aligned with the zygomatic arch. 0.6 mm thick sections were obtained helically utilizing a  $512 \times 512$  matrix, and a field of view of 22 cm resulting in a voxel size of  $0.43 \times 0.43 \times 0.6$  mm. Sagittal and coronal reconstructed images were performed from this data. This same scanner was used to obtain images for conversion into a surgical simulation program developed by the Ohio Supercomputer Center / Ohio State University (OSC/OSU) (Columbus, OH).

Imaging data was stored in digital imaging and communications in DICOM format and subsequently analyzed using an open source picture archiving and communication system (PACS) software, OsiriX Imaging Software (OsiriX Foundation, Geneva, Switzerland). Standard measurements of the maximum height (vertical distance between the jugulo-

carotid notch and the basal turn of the cochlea) and width (maximum horizontal distance between the internal carotid artery and either jugular bulb or posterior fossa dural plate when taken at a tangent to the basal turn of the cochlea) of the infracochlear approach were taken on the parasagittal images. Axial images were used to measure the depth of this approach (maximum distance of a path parallel to the line of the external auditory canal from the promontory to the posterior fossa dural plate or medial limit of the petrous temporal bone) (Figures 1 and 2).

In addition, the maximum diameter of a circular fenestration that could be created in the infracochlear space without breaching the basal turn of the cochlea, internal carotid artery, or the jugular bulb was used to simulate a computer-assisted drill path. A further measurement of the horizontal distance between the jugular bulb and internal carotid artery was taken at the equator of this circular fenestration (Figures 1 and 2). All measurements were taken using the region of interest (ROI) tools in the OsiriX imaging software. Temporal bones were noted to have either pneumatized or non-pneumatized petrous apices.

The collected data was stored and analyzed in Microsoft Excel 2007 (Microsoft Corporation, Redmond, WA, USA). A Student t-test was used to analyze whether there was any significant difference in diameter of the virtual circular fenestration between temporal bones with pneumatized or non pneumatized petrous apices. Institutional review board approval was not required for this study since only cadaveric specimens were used.

For the 2<sup>nd</sup> phase of the study, the HRCT digitized images of the cadaveric specimens were processed by the OSC/OSU team to create a virtual temporal bone, allowing the infracochlear approach to be performed with the simulator. The approach involved only bone work (no soft tissue structures were present, such as ear canal skin or the tympanic membrane). The bone work included a bony canalplasty that was wide enough to allow the identification of the round window and hypotympanum. In addition, the OSC/OSU simulator allowed the use of an anatomy guide, allowing the color-coded identification of the 3 important neurovascular structures to be avoided during drilling (red-cochlea, brown-internal carotid artery, green- jugular bulb). In addition, the simulator allowed slicing of planes and adjustment of bone transparency in 3 dimensions. The canalplasty was performed with cutting and diamond burrs as deemed necessary. The infracochlear approach into the petrous apex was performed with a 2mm diamond. Manipulation and rotation of the temporal bone in 3-dimensional space was performed to locate the burr and assess if neurovascular injury had occurred and if adequate penetration into the petrous apex had occurred.

## Results

HRCT scans were performed on 102 cadaveric skulls. (total of 204 temporal bones). The results of the radiographic measurements of mean height, width, depth, width at equator, diameter and area of a virtual circular fenestration are presented in Table 1, along with the respective standard deviation and 95% confidence intervals for the means.

Analysis of the difference between the mean diameter of the circular fenestra in pneumatized (5.7 +/- 0.6mm) and non pneumatized (5.1 +/- 0.4mm) petrous temporal bones by an unpaired t-Test yielded a statistically significant result ( $p = 0.04$ ) In the surgical simulation program, the time to perform the infracochlear approach ranged from 3.1 – 12.6 minutes (mean: 6.1 minutes). Although it appeared with each virtual bone that the petrous apex had been reached via the infracochlear route, it was difficult at times to tell if injury had occurred to the cochlea, internal carotid artery, or jugular bulb. The time to perform the same approach on the cadaveric bone ranged from 4.32 – 14.1 minutes (mean 9.3 minutes).

Due to the small sample size, statistical evaluation was not performed of the virtual and cadaveric infracochlear approach surgical times.

## Discussion

The surgical approach to the petrous apex via the transcanal infracochlear route has been previously described by Giddings et. al<sup>4</sup>. The procedure involves identification of the internal carotid artery and jugular bulb with gradual enlargement of the surgical window inferior to the basal turn of the cochlea. Through exposure of these structures, potential vascular injury and sensorineural hearing loss may result; however, minimal morbidity related to this approach has been reported.<sup>5,6</sup> CAS has the potential advantage of improved surgical precision and accuracy<sup>2,3</sup>, with the possibility of an integrated image guidance platform. This would allow the surgeon to drill a precise predetermined opening into narrow surgical corridors, an application that may have a role in the infracochlear approach to the petrous apex. The advantage being that neither the cochlea, jugular bulb, nor carotid would need to be exposed.

Our approach was to determine the maximum size circular fenestration that would mimic an opening created by a round diamond burr. The maximum sized circle that could be placed without violating the cochlea, jugular bulb, or internal carotid artery would represent the largest sized diameter circular fenestration possible in that particular temporal bone. The result being that a smaller sized circular fenestration based on the previous measurement would therefore provide a path that allows for a margin for error when applied to a robotic arm. In this study, we found temporal bones with pneumatized petrous apices have an overall larger infracochlear space. The mean diameter of a circular infracochlear path was 5.1 and 5.7 mm in non-pneumatized and pneumatized bones, respectively. However, the smallest diameter noted in our study was 2.8mm. Thus, a 2mm burr should be sufficiently small to avoid damage to vital structures. The question that is not answered is whether this would be of potentially sufficient size to allow drainage of the petrous apex since only cadaveric and virtual infracochlear approaches were performed and no actual patient data was evaluated.

Giddings et. al.<sup>4</sup> reported a mean area of infracochlear fenestrae of 25.6 +/- 16.3mm<sup>2</sup>. The fenestrae in this and other studies were shaped according to the anatomy of the infracochlear space and varied between triangular and rectangular shapes. Area calculations were estimated using standard rectangular and triangular area formulae. This is nevertheless comparable to the area of the circular fenestrae we found in the present study being 21.5 and 27.8mm<sup>2</sup> in non-pneumatized and pneumatized bones, respectively. The use of a circular shape to enter this space therefore would appear not to underestimate the available space in this infracochlear compartment to any great degree, when compared to the use of a variable shaped polygon to contour to the carotid, jugular bulb and basal turn of cochlear in estimating the space available for drilling in this area. Comparisons of our standard measurements of height (jugulocarotid notch to basal turn of cochlear) and width (jugular bulb to carotid taken at a tangent to the basal turn of the cochlea) were comparable to those found in other anatomical studies<sup>4,8</sup>. Extracting from data presented by Gidding et. al. revealed a height and width of 5.3 and 6.1mm in 10 temporal bones. Haberkamp<sup>8</sup> in 20 temporal bones found measurements of 7.33 and 9.41. However Gerek et al.<sup>7</sup> in 6 temporal bones found height and widths of 3.2 and 4.7mm respectively, smaller than the present and previous studies. Their approach differed from previous reports and also from the present study in that they used an anterior modification to the fenestra (transcanal anterior approach), to avoid injury to the round window and jugular bulb. The location of the fenestra studied by Gerek's group was more anteriorly located in relation to the cochlea, which may explain the difference in dimensions found when compared to this current and

prior studies. In this current series of 204 temporal bones, we found these distances to be 7.2 and 9.5mm in non pneumatized bones and 7.6 and 10.1 in pneumatized bones, demonstrating that the infracochlear route affords sufficiently large dimensions to consider the application in computer assisted surgery, even when allowing for a margin of error in robotic translational movements.

Future application of this study will involve the mating of the robotic arm with the surgical simulator and image guidance to drill a fenestra in the infracochlear space. By using measurements from this present radiographic study, a 2mm burr is beyond the 95% confidence interval for the diameter of the circular fenestra that could safely be accommodated in the infracochlear space. The challenge will be the guidance of a robotic arm which due to the lack of a readily compatible image guidance platform that interfaces with existing robotic systems, will necessarily be guided by a human operator. Ultimately, it can be envisaged that this approach could be performed by an autonomous or semi-autonomous robotic system.

Use of surgical simulators will grow in importance, particularly as the cost of obtaining cadaveric specimens and maintaining a temporal bone lab is prohibitive for most hospitals outside academic centers; religious and cultural objections to the use of cadaveric and animal specimens also exist<sup>9</sup>. Although the current simulator did show the ability to perform an infracochlear approach, the limitations included a resolution of 2mm, which made it difficult to assess if neurovascular injury could have occurred. However, future improvements in the system will incorporate ultra-high resolution CT and MRI imagery, allowing resolution of several hundred micrometers<sup>10</sup>. Current problems with the simulator include lack of true depth perception, lack of realistic tactile (haptic) feedback, and lack of soft tissue detail (e.g., for creation of hypotympanotomy flap and soft-tissue canalplasty). However, benefits included ability to visualize and manipulate the temporal bone in 3 dimensional space with labeling of important anatomic structures. Surgical path planning for novice (e.g., residents in training), inexperienced, or occasional surgeons (general otolaryngologist) is clearly an asset (as well as for neurotologists performing revision cases or difficult cases). As the OSC/OSU simulator continues to improve, future versions will include use of suction-irrigation and active bleeding. In addition, the ability to perform measurements with the simulator and having a simultaneous view of important neurovascular structures during the drilling will improve teaching of novice surgeons and reduce the intraoperative risk of morbidity and mortality.

In conclusion, temporal bones with pneumatized petrous apices have an overall larger infracochlear space. Although the mean diameter of a circular infracochlear path that would avoid damage to vital structures was sufficiently large in both pneumatized and non-pneumatized petrous apices to have a potential application as a safe approach in robotic surgery, variations requiring a smaller burr do exist. Such an application is feasible with mating of a robotic system with CT or MRI guided imagery and the surgery simulator, which is the next phase of this study.

## References

1. Isaacson B, Kutz JW, Roland PS. Lesions of the petrous apex: diagnosis and management. *Otolaryngol Clin North Am.* 2007; 40(3):479–519. [PubMed: 17544693]
2. Menon M, Tewari A, Peabody JO, Shrivastava A, Kaul S, Bhandari A, Hemal AK. Vattikuti Institute prostatectomy, a technique of robotic radical prostatectomy for management of localized carcinoma of the prostate: experience of over 1100 cases. *Urol Clin North Am.* Nov; 2004 31(4): 701–17. [PubMed: 15474597]

3. Nifong LW, Chitwood WR, Pappas PS, Smith CR, Argenziano M, Starnes VA, Shah PM. Robotic mitral valve surgery: a United States multicenter trial. *J Thorac Cardiovasc Surg.* Jun; 2005 129(6): 1395–404. [PubMed: 15942584]
4. Giddings NA, Brackmann DE, Kwartler JA. Transcanal infracochlear approach to the petrous apex. *Otolaryngol Head Neck Surg.* 1991; 104:29–36. [PubMed: 1900626]
5. Brackmann DE, Toh EH. Surgical management of petrous apex cholesterol granulomas. *Otol Neurotol.* 2002; 23:529–33. [PubMed: 12170157]
6. Mosnier I, Cyna-Gorse F, Grayeli AB, et al. Management of cholesterol granulomas of the petrous apex based on clinical and radiological evaluation. *Otol Neurotol.* 2002; 23:522–8. [PubMed: 12170156]
7. Gerek M, Satar B, Yazar F, Ozan H, Ozkaptan Y. Transcanal anterior approach for cystic lesions of the petrous apex. *Otol Neurotol.* 2004; 25(6):973–6. [PubMed: 15547428]
8. Haberkamp TJ. Surgical anatomy of the transtemporal approaches to the petrous apex. *Am J Otol.* 1997; 18:501–6. [PubMed: 9233493]
9. Stredney D, Hittle B, Collidas J, McLoughlin MA. Translating human simulation technologies to veterinary surgical training: accelerating adoption. *Stud Health Technol Inform.* 2008; 132:502–4. [PubMed: 18391355]
10. Wiet GJ, Schmalbrock P, Powell K, Stredney. Use of ultra-high resolution data for temporal bone dissection simulation. *Otolaryngol Head Neck Surg.* Dec; 2005 133(6):911–5. [PubMed: 16360513]

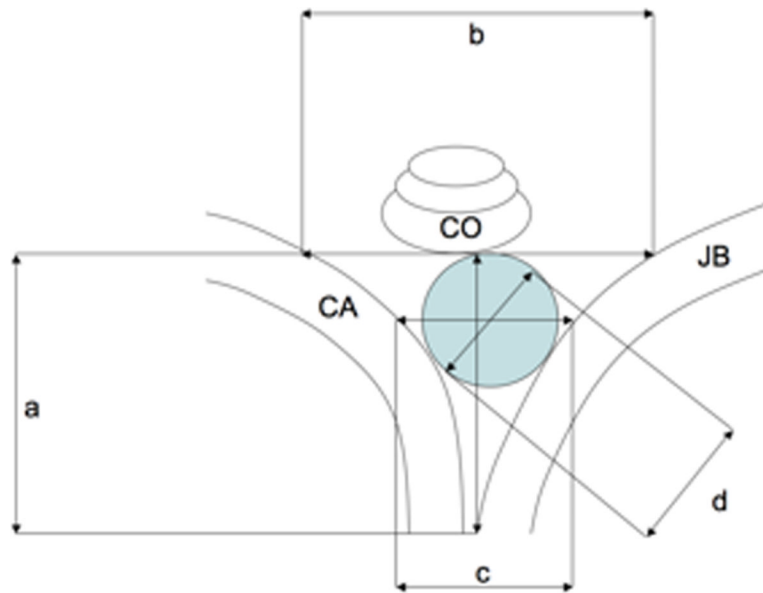


**Figure 1.** Schematic representation of measurements taken from HRCT scans. a) Height, b) Width, c) Width at equator of circular fenestration, d) Diameter of circular fenestration; CA, Carotid artery; CO, Cochlea; JB, Jugular Bulb; shaded area represents area of circular fenestration.

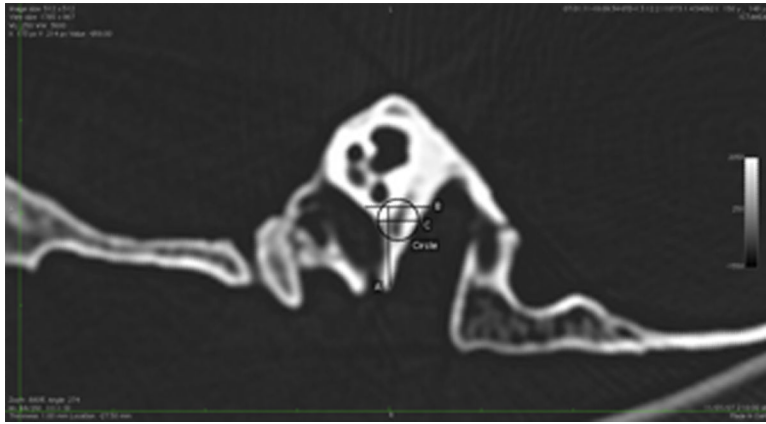


**Figure 2.** Parasagittal HRCT image to illustrate measurements taken. Measurements are shown in Table 1.



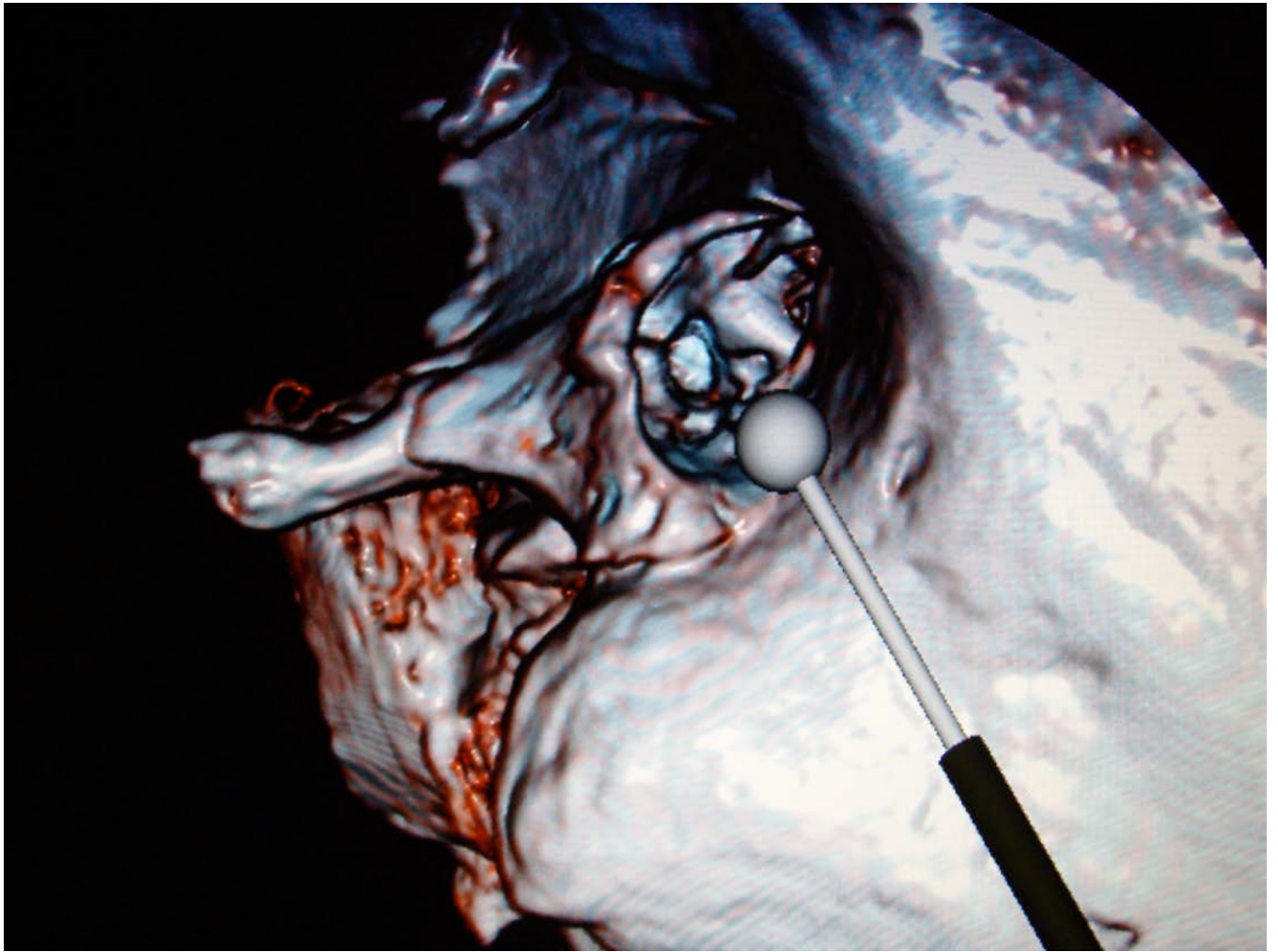




**Figure 3A and B.** Simulated views of left infracochlear approach using OSC/OSU simulator in normal view (A) and with increased transparency and depth of image, allowing simultaneous visualization of internal carotid artery, jugular bulb, and cochlea.

**Table 1**

Radiographic Measurements

Measurement	Non-pneumatized petrous apex					Pneumatized petrous apex				
	Mean	Minimum	Maximum	Standard deviation	95 % Confidence interval of mean	Mean	Minimum	Maximum	Standard deviation	95 % Confidence interval of mean
Height	7.2	4.8	10.2	1.3	6.8 - 7.6	7.6	5.5	11.3	1.3	7.2 - 8.0
Width	9.5	5.0	15.4	2.6	8.7 - 10.3	10.1	5.5	15.3	3.1	9.1 - 11.1
Width at equator	6.7	3.0	14.0	3.0	5.7 - 7.6	7.5	14.5	3.1	3.3	6.4 - 8.6
Diameter circle	5.1	2.8	9.3	1.2	4.7 - 5.5	5.7	3.1	9.4	1.7	5.1 - 6.3
Area circle mm <sup>2</sup>	21.5	6.1	67.3	10.9	18.1 - 24.9	27.8	7.4	69.0	16.4	22.2 - 33.4
Depth	17.4	1.7	23.0	3.3	16.4 - 18.4	18.6	14.3	23.8	2.4	17.8 - 19.4